Syntheses, Structures, and Spectroscopic Studies of Several New Classes of Compounds Having Boron–Arsenic Bonds

Mark A. Petrie, Marilyn M. Olmstead, H. Hope, Ruth A. Bartlett, and Philip P. Power*

Contribution from the Department of Chemistry, University of California, Davis, California 95616

Received September 14, 1992

Abstract: Several new arsinoboranes, wherein boron and arsenic are three coordinate, have been prepared and characterized. They are analogous to B–N and B–P species in which p–p π-bonding, involving the pnictide lone pair and the empty boron p-orbital, may occur. The main conclusion of these studies is that B–As π-bonding, although inherently strong, is difficult to achieve because of the larger inversion barrier at arsenic. Nontheless, very electropositive or bulky substituents at arsenic reduce this barrier sufficiently to observe substantial B–As π-interactions. The compounds studied include $[PhB(Cl)As(t\text{-}Bu)_2]_2$ (**1**), $PhB\{As(t\text{-}Bu)_2\}_2$ (**2**), $Cp^*B(Cl)As(t\text{-}Bu)_2$ (**3**), $(C_{20}H_{30})BAs(t\text{-}Bu)_2$ (**4**), $Mes_2BAsPhLi(THF)_3$ (**5**), $[Mes_2BAsPh][Li(TMEDA)_2]$ (**6**), and $Mes_2BAs(Ph)SiMe_3$ (**7**) (Cp^* = pentamethylcyclopentadienyl, TMEDA = *N,N,N'N'*-tetramethylenediamine, Mes = 2,4,6-$Me_3C_6H_2$). The species **5** and **6** have been reported in a preliminary note. All compounds were characterized by X-ray crystallography and ^1H NMR and ^{11}B NMR spectroscopy. In addition, **5** and **7** were characterized by variable-temperature ^1H NMR studies.

Introduction

Boron–nitrogen compounds have enjoyed a widespread interest due, in part, to their isoelectronic relationship to carbon species.[1,2] In contrast, work on compounds having bonds between boron and the heavier pnictides, i.e., P, As, and Sb, has been much slower to develop.[3,4] In fact, it is only since the mid-1980s that π-bonding has been firmly established in species such as the B–P analogues of ethylene ($R_2BPR'_2$),[5a] the allyl cation ($RP(BR'_2)_2$),[5b] and borazine, ($\{RBPR'\}_3$).[5c,d] The main feature of interest has been the variation of the interaction between the phosphorus lone pair and the empty p-orbital of boron.[6] Until recently, these studies had not been extended to B–As species. In fact, few[8-11] structures of molecular compounds with B–As bonds have been determined since the structure of boron arsenide (BAs)[7] was published. In two of these more recent reports, coordination numbers greater than three at B and As, as in the closo icosahedral species $MAs_2B_9H_{8\text{ or }9}$ (where M = Pt or Pd)[8] or the adducts Me_3AsBX_3 (where X = Cl, Br, and I),[9] preclude the possibility of significant B–As π-bonding. Another paper, however, concerned the Zintl compound, K_3BAs_2,[10] whose structure involves a linear $[As–B–As]^{3-}$ array with short (1.868 Å) B–As bonds. The molecular species most related to compounds in this paper is the cyclic derivative $[\text{-}B(Ni\text{-}Pr_2)\text{-}N(t\text{-}Bu)\text{-}B(Ni\text{-}Pr_2)\text{-}As(Ph)]$(**8**), in which there is competition for the empty boron p-orbital between the nitrogen and arsenic lone pairs.[11] The short exocyclic B–N distances (1.40 Å) and near coplanarity of the coordination environments at boron and nitrogen suggest that B–N π-bonding is dominant. This view is confirmed by the normal B–As single bond lengths (2.06 Å, identical to the sum of the B and As radii[12]) and the pyramidicity of the arsenic center ($\Sigma° = 272°$). Very recently, this group characterized $Mes_2BAsPhLi(THF)_3$ (**5**) and the solvent-separated ion pair $[Mes_2BAsPh][Li(TMEDA)_2]$ (**6**)[4] which were shown to have multiple bonds between boron and arsenic. In order to study the factors that control B–As π-bonding, the synthesis, structural (X-ray), and spectroscopic (^{11}B and variable-temperature ^1H NMR) characterization of several new classes of boron–arsenic compounds are now described. In considering the bonding in these compounds it should be borne in mind that there is a significant difference in radius between B (0.85 Å) and As (1.21 Å).[12] However, the polarity of the B–As pair, as expressed by the difference in electronegativity between the two atoms, is relatively small: 2.01 for B and 2.2 for As.[13] Another important consideration is the size of the inversion barrier at arsenic which is usually quite large (>40 kcal mol^{-1})[14] and is expected to strongly affect the extent of multiple bonding in these compounds.

Experimental Section

General Procedures. All experiments were performed either by using modified Schlenk techniques or in a Vacuum Atmospheres HE 43-2 drybox under nitrogen. Solvents were freshly distilled from a sodium–potassium alloy and degassed twice prior to use. ^{11}B and ^1H NMR spectra were recorded in C_6D_6 or C_7D_8 solutions using a General Electric QE-300 spectrometer. The compounds $t\text{-}Bu_2AsH$,[15] $PhBCl_2$,[16] Cp^*BCl_2,[17] Cp^*_2BCl,[17] and Mes_2BF[18] were synthesized according to literature methods. $PhAsH_2$ was obtained by reduction of $PhAsO(OH)_2$ (Aldrich) with zinc amalgam.[19]

(1) Niedenzu, K.; Dawson, J. W. *Boron–Nitrogen Compounds*; Springer-Verlag: Berlin, 1964.
(2) Lappert, M. F.; Power, P. P.; Sanger, A. R.; Srivastava, R. C. *Metal and Metalloid Amides*; Ellis-Horwood: Chichester, 1979.
(3) Wasson, J. R. *Gmelin Handbuch der Anorganischen Chemie, Ergänzungswerk zur 8. Aufl Bd. 19, Borverbindungen, Teil 3*; Springer: Berlin, 1975; p 93. Power, P. P. *Angew. Chem., Int. Ed. Engl.* **1990**, *29*, 449.
(4) Petrie, M. A.; Shoner, S. C.; Dias, H. V. R.; Power, P. P. *Angew. Chem., Int. Ed. Engl.* **1990**, *29*, 1033.
(5) (a) Feng, X.; Olmstead, M. M.; Power, P. P. *Inorg. Chem.* **1986**, *25*, 4616. (b) Bartlett, R. A.; Dias, H. V. R.; Power, P. P. *Inorg. Chem.* **1988**, *27*, 3919. (c) Dias, H. V. R.; Power, P. P. *Angew. Chem., Int. Ed. Engl.* **1987**, *26*, 1270. (d) Dias, H. V. R.; Power, P. P. *J. Am. Chem. Soc.* **1989**, *111*, 144.
(6) Pestana, D. C.; Power, P. P. *J. Am. Chem. Soc.* **1991**, *113*, 8426.
(7) Perri, J. A.; La Placa, S.; Post, B. *Acta Crystallogr.* **1958**, *11*, 310.
(8) McGrath, M.; Spalding, T. R.; Fontaine, X. L. R.; Kennedy, J. D.; Thornton-Pett, M. *J. Chem. Soc., Dalton Trans.* **1991**, 3223.
(9) Chadha, R. K.; Chehayber, J. M.; Drake, J. E. *J. Crystallogr. Spectrosc. Res.* **1985**, *15*(1), 53.
(10) von Schnering, H.-G.; Somer, M.; Hartweg, M.; Peters, K. *Angew. Chem., Int. Ed. Engl.* **1990**, *29*, 65.
(11) van Bonn, K.-H.; Schreyer, P.; Paetzold, P.; Boese, R. *Chem. Ber.* **1988**, *121*, 1045.
(12) Covalent radii estimated from homonuclear bond lengths: Sutton L., Ed.; Tables of Interatomic Distances and Configuration in Molecules and Ions. *Spec. Publ. Chem. Soc.* **1958**, *11*; *Spec. Publ. Chem. Soc.* **1965**, *18*. Slater, J. C. *J. Chem. Phys.* **1964**, *41*, 3199.
(13) Allred, A. L.; Rochow, E. G. *J. Inorg. Nucl. Chem.* **1958**, *5*, 264.
(14) Mislow, K. *Trans. N.Y. Acad. Sci.* **1973**, *35*(3), 227.
(15) Tzschach, V. A.; Deylig, W. *Z. Anorg. Allg. Chem.* **1965**, *336*, 36.
(16) Triechel, P. M.; Benedict, J.; Haines, R. G. *Inorg. Synth.* **1972**, *13*, 32.
(17) Jutzi, P.; Krato, B.; Hursthouse, M.; Howes, A. J. *Chem. Ber.* **1987**, *120*, 565.
(18) The synthesis is identical to that described for $(2,6\text{-}Me_2C_6H_3)_2BF$ in: Chen, H.; Bartlett, R. A.; Olmstead, M. M.; Power, P. P.; Shoner, S. C. *J. Am. Chem. Soc.* **1990**, *112*, 1048.
(19) Palmer, C. S.; Adams, R. *J. Am. Chem. Soc.* **1922**, *44*, 1356.

0002-7863/93/1515-3221$04.00/0 © 1993 American Chemical Society

Table I. Selected Crystallographic Data and Structural Parameters for 1–4[a] and 7[b]

	1	2	3	4	7
formula	$C_{28}H_{46}B_2Cl_2As_2$	$C_{22}H_{41}BAs_2$	$C_{18}H_{33}BClAs$	$C_{28}H_{48}BAs$	$C_{27}H_{36}BAsSi$
formula weight	625	466.2	370.6	470.4	474.4
T, K	130	130	130	130	130
crystal system	monoclinic	triclinic	monoclinic	triclinic	monoclinic
a, Å	9.567(2)	9.321(2)	9.382(5)	8.902(3)	20.714(9)
b, Å	9.453(2)	9.329(2)	15.103(4)	11.457(4)	9.894(5)
c, Å	16.562(3)	15.185(2)	14.082(5)	14.381(4)	26.375(10)
α (deg)		96.05(1)		104.89(2)	
β (deg)	101.72(1)	104.17(1)	99.91(3)	96.66(3)	102.42(3)
γ (deg)		104.33(1)		110.31(2)	
V, Å^3	1471.3(4)	1220.9(4)	1965.7(14)	1294.9(7)	5279(4)
space group	$P2_1/n$	$P\bar{1}$	$P2_1/n$	$P\bar{1}$	$P2_1/n$
Z	4	2	4	2	8
D_{calc} (g cm^{-3})	1.411	1.268	1.252	1.206	1.194
μ (mm^{-1})	4.642	2.733	3.544	1.828	1.338
2θ range (deg)	0–115	0–115	0–115	0–115	0–45
no. of obsvd reflcns	1862, $I > 2\theta(I)$	3225, $I > 2\sigma(I)$	2429, $I > 2\sigma(I)$	3348, $I > 2\sigma(I)$	4176, $I > 2\sigma(I)$
no of variables	154	226	190	271	541
R, R_w	0.045, 0.055	0.051, 0.074	0.041, 0.048	0.047, 0.058	0.053, 0.046

[a] Data were collected with Cu Kα radiation (λ = 1.541 84 Å). [b] Data were collected with Mo Kα radiation (λ = 0.710 69 Å).

Synthesis. [PhB(Cl)As(*t*-Bu)$_2$]$_2$ (1). A rapidly stirred solution of *t*-Bu$_2$AsH (0.50 g, 4.2 mmol) in Et$_2$O (30 mL) was treated dropwise with *n*-BuLi (2.6 mL, 1.6 M in hexanes) with cooling in an ice bath. After being stirred for 30 min, this solution was added dropwise to PhBCl$_2$ (0.67 g, 4.2 mmol) in hexane (20 mL). The yellow solution was stirred overnight, after which all volatile compounds were removed under reduced pressure. The residue was taken up in hexane (20 mL), filtered, and concentrated. Slow cooling in a −20 °C freezer afforded the product as yellow crystals: yield 0.79 g, 60%; mp 81–85 °C; ^{11}B NMR (C$_6$D$_6$) δ 83.0; ^{1}H NMR (C$_6$D$_6$) δ 1.13 (s, -CMe$_3$), 6.89 (m, Ph), 8.01 (d, Ph).

PhB{As(*t*-Bu)$_2$}$_2$ (2). An Et$_2$O (30 mL) solution of *t*-Bu$_2$AsLi (prepared from *t*-Bu$_2$AsH (0.43 g, 2.3 mmol) and 1.6 M *n*-BuLi in hexanes (1.4 mL, 2.3 mmol)) was added via cannula to **1** (0.73 g, 1.1 mmol) in hexane (20 mL). After overnight stirring, the solvents were removed under reduced pressure and the residue was extracted with hexane (20 mL). The solution was then filtered and concentrated to ca. 5 mL. Yellow-orange plates of **2** separated from solution when stored overnight in a −20 °C freezer: yield 0.48 g, 46%; mp 68–72 °C; ^{11}B NMR (C$_6$D$_6$) δ 107.6; ^{1}H NMR (C$_6$D$_6$) δ 1.21 (s, -CMe$_3$), 6.95 (m, Ph), 7.06 (d, Ph).

Cp*B(Cl)As(*t*-Bu)$_2$ (3). The dropwise addition of *t*-Bu$_2$AsLi (prepared from *t*-Bu$_2$AsH (0.57 g, 3 mmol) in Et$_2$O (30 mL) and 1.6 M *n*-BuLi in hexanes (1.9 mL, 3 mmol)) to Cp*BCl$_2$ (0.65 g, 3 mmol) in hexane (20 mL) gave a cloudy orange-red solution. After the solution was stirred for 12 h, all volatile components were removed under reduced pressure. The residue was taken up in pentane (15 mL), and the solution was filtered. Slow cooling in a −20 °C freezer afforded orange crystals: yield 0.42 g, 38%; mp 100–108 °C; ^{11}B NMR (C$_6$D$_6$) δ 69.6; ^{1}H NMR (C$_6$D$_6$) δ 1.26 (S, -CMe$_3$), 1.71 (S, Me$_5$C$_5$).

(C$_{20}$H$_{30}$)BAs(*t*-Bu)$_2$ (4). Cp*$_2$BCl (0.63 g, 2 mmol) in hexane (20 mL) was added to *t*-Bu$_2$AsLi (prepared from *t*-Bu$_2$AsH (0.38 g, 2 mmol) and 1.6 M *n*-BuLi in hexanes (1.3 mL, 2 mmol)) in Et$_2$O (40 ml). The solution was refluxed for 12 h, after which all volatile materials were removed. The residue was dissolved in pentane (20 mL) and filtered. Slow cooling of the yellow-green solution in a −20 °C freezer gave the product as yellow crystals: yield <20%; ^{11}B NMR (C$_6$D$_6$) δ 52.1; ^{1}H NMR (C$_6$D$_6$) δ 1.44 (S, -CMe$_3$), 1.63–1.75 (C$_{20}$H$_{30}$, -Me).

Mes$_2$BAsPhLi(THF)$_3$ (5).[4] Compound **5** was prepared by the addition of Mes$_2$BF (1 g, 3.7 mmol) to a solution of Li$_2$AsPh[20] (0.62 g, 3.7 mmol) in THF (50 mL). The red solution was stirred for 3 h, and the solvent was removed under reduced pressure. The residue was dissolved in Et$_2$O (25 mL), filtered, and cooled in a −20 °C freezer over 10 h. The resultant orange-red crystals were isolated by filtration: yield 1.4 g, 5%; mp 111–114 °C; ^{11}B NMR (C$_6$D$_6$) δ 74.6; ^{1}H NMR (in xylene-d_{10}) δ 1.4 (m, THF), 2.25 (s, *p*-Me), 2.57 (s, *o*-Me), 2.73 (s, *o*-Me), 3.45 (m, THF), 6.77 (s, *m*-H), 6.9 (m, Ph), 7.42 (m, Ph).

[Mes$_2$BAsPh][Li(TMEDA)$_2$] (6).[4] Two equivalents of TMEDA (0.18 g, 0.24 mL, 3.2 mmol) were added to an Et$_2$O (20 mL) solution of (**5**) (0.99 g, 1.6 mmol). The mixture was stirred for 5 min, a finely divided yellow precipitate appeared. Addition of THF (3–4 mL) resulted in a clear solution, and cooling in a −20 °C freezer for 10 h gave the product as orange-red crystals: yield 0.37 g, 36%; mp >140 °C dec (slow); ^{11}B NMR (C$_6$D$_6$) δ 74.9; ^{1}H NMR (in xylene-d_{10}) δ 1.86 (s, Me$_2$N), 1.896 (s, CH$_2$N), 2.24, 2.25 (s, *p*-Me), 2.663, 2.868 (*s*, *o*-Me), 6.87, 6.93 (m, CH), 7.06 (m, Ph), 7.76 (d, Ph).

Mes$_2$BAs(Ph)SiMe$_3$ (7) Compound **5** (1.6 g, 2.5 mmol) dissolved in Et$_2$O (20 mL) at −10 °C was treated with Me$_3$SiCl (0.25 g, 2.5 mmol) via syringe. A white precipitate appeared immediately, and the solution was warmed to 0 °C over 1 h. Solvents were removed at this temperature. The yellow solid was dissolved in pentane (20 mL), filtered, and cooled to −20 °C overnight. Yellow crystalline aggregates of the product appeared over 2 days: yield 0.86 g, 72%; mp >107 °C dec (slow); ^{11}B NMR (C$_7$D$_8$) δ 92.5; ^{1}H NMR (C$_7$D$_8$) δ 0.253 (s, SiMe$_3$), 2.12 (s, *p*-Me), 2.32 (s, *o*-Me), 6.63 (s, *m*-H of Mes), 6.92 (m, Ph) 7.15 (d, Ph).

X-ray Data Collection and the Solution and Refinement of the Structures. Crystals of **1–7** were coated with a layer of hydrocarbon oil upon removal from the Schlenk tube. A suitable crystal was selected, attached to a glass fiber by silicon grease, and immediately placed in the low-temperature N$_2$ stream.[21] X-ray data were collected with a Siemens R3 m/V diffractometer equipped with a graphite monochromator and a locally modified Enraf–Nonius LT apparatus. Calculations were carried out on a Microvax 3200 computer using the SHELXTL PLUS program system. Neutral atom scattering factors and the correction for anomalous dispersion were from ref 22. The structures of all molecules were solved by direct methods. Details of data collection and refinement are provided in Table I. Important bond distances and angles for the molecules **1–4** and **7** are provided in Table II.

Results

Structural Descriptions. The structures of **1–4** and **7** are described here. Those of compounds **5** and **6** (Figures 5 and 6) were reported in a preliminary communication.[4] Selected structural parameters for **1–7** and other related compounds are summarized in Table III.

[PhB(Cl)As(*t*-Bu)$_2$]$_2$ (1). The molecular structure of **1**, which is illustrated in Figure 1, consists of a dimer with distorted tetrahedral geometries at boron and arsenic. The molecule is located on an inversion center. The As$_2$B$_2$ core of the molecule is therefore planar and has slightly different B–As bond lengths of 2.200(5) and 2.184(5) Å. The mean As–C bond length is 2.035(4) Å, and the B–C(1) and B–Cl bond lengths are 1.580(6) and 1.871(5) Å, respectively. Within the As$_2$B$_2$ core the B–As–B′ and As–B–As′ angles are 91.4(2)° and 88.6(2)°, and the separation of the two As atoms is 3.061 Å. The C(7)–As–C(11) angle is 106.9(2)°, while the Cl–B–C(1) angle is slightly narrower, 105.6(3)°.

(20) Tzschach, A.; Pacholke, G. *Chem. Ber.* **1964**, *97*, 419.
(21) This method is described in: Hope, H. *Experimental Organometallic Chemistry: A Practicum in Synthesis and Characterization*; Wayda, A. L., Darensbourg, M. Y., Eds.; ACS Symposium Series 357, American Chemical Society: Washington DC, 1987; Chapter 10.
(22) *International Tables for X-Ray Crystallography*; Kynoch Press: Birmingham, England, 1974; Vol. IV.

Table II. Important Bond Distances (Å) and Angles (deg) for **1–4** and **7**

bond lengths (Å)		bond angles (deg)	
		1	
As–B	2.200(5)	B–As–As′	91.4(2)
As–B′	2.184(5)	C(7)–As–C(11)	106.9(2)
As–C(7)	2.037(4)	As–B–As′	88.6(2)
As–C(11)	2.033(4)	Cl–B–C(1)	105.6(3)
B–Cl	1.871(5)		
B–C(1)	1.580(6)		
		2	
As(1)–B	2.064(5)	C(15)–As(1)–B	106.9(2)
As(2)–B	2.034(5)	C(19)–As(1)–B	100.6(2)
As(1)–C(15)	2.028(4)	C(15)–As(1)–C(19)	109.0(2)
As(1)–C(19)	2.046(4)	C(7)–As(2)–B	108.7(2)
As(2)–C(7)	2.047(5)	C(11)–As(2)–B	103.8(2)
As(2)–C(11)	2.026(4)	C(7)–As(2)–C(11)	107.9(2)
B–C(1)	1.562(7)	As(1)–B–As(2)	114.0(2)
		As(1)–B–C(1)	124.3(3)
		As(2)–B–C(1)	121.6(3)
		3	
As–B	2.085(4)	B–As–C(1)	102.7(1)
As–C(1)	2.028(4)	B–As–C(5)	101.9(1)
As–C(5)	2.029(4)	C(1)–As–C(5)	107.1(1)
B–C(9)	1.596(6)	As–B–C(9)	123.8(2)
B–Cl	1.776(4)	As–B–Cl	121.0(2)
		Cl–B–C(9)	115.0(3)
		4	
As–B	2.084(4)	C(13)–C(14)	1.515(6)
As–C(21)	2.028(4)	C(14)–C(15)	1.590(6)
As–C(25)	2.031(4)	C(11)–C(15)	1.571(5)
B–C(1)	1.611(6)	C(2)–C(14)	1.583(4)
B–C(11)	1.609(5)	C(5)–C(15)	1.574(4)
C(1)–C(2)	1.585(5)		
C(2)–C(3)	1.532(6)	B–As–C(21)	104.3(2)
C(3)–C(4)	1.325(6)	B–As–C(25)	111.0(2)
C(4)–C(5)	1.527(5)	C(21)–As–C(25)	106.8(1)
C(1)–C(5)	1.561(6)	As–B–C(1)	136.2(2)
C(11)–C(12)	1.535(6)	As–B–C(11)	118.3(3)
C(12)–C(13)	1.323(5)	C(1)–B–C(11)	105.5(3)
		5	
As–B	1.926(6)	B–As–Li	122.7(2)
As–Li	2.670(9)	B–As–C(19)	107.8(2)
As–C(19)	1.957(5)	Li–As–C(19)	110.9(2)
B–C(1)	1.613(7)	As–B–C(1)	115.1(3)
B–C(10)	1.588(7)	As–B–C(10)	124.6(4)
Li–O(1)	1.939(9)	C(1)–B–C(10)	120.3(4)
Li–O(2)	1.940(10)		
Li–O(3)	1.945(9)		
		6	
As–B	1.936(11)	B–As–C(19)	107.1(4)
As–C(19)	1.925(9)	As–B–C(1)	114.8(6)
B–C(1)	1.612(16)	As–B–C(10)	126.4(8)
B–C(10)	1.595(13)	C(1)–B–C(10)	118.7(8)
Li–N(1)	2.097(18)		
Li–N(2)	2.146(19)		
Li–N(3)	2.112(19)		
Li–N(4)	2.085(18)		
		7	
As(1)–B(1)	2.031(8)	B(1)–As(1)–C(1)	107.9(3)
As(1)–Si(1)	2.366(3)	Si(1)–As(1)–B(1)	106.8(2)
As(1)–C(1)	1.954(7)	Si(1)–As(1)–C(1)	107.7(2)
B(1)–C(10)	1.569(10)	As(1)–B(1)–C(10)	115.9(5)
B(1)–C(19)	1.584(10)	As(1)–B(1)–C(19)	119.2(5)
As(2)–B(2)	1.999(8)	C(10)–B(1)–C(19)	124.4(6)
As(2)–Si(2)	2.365(3)	B(2)–As(2)–C(28)	106.1(3)
As(2)–C(28)	1.941(7)	Si(2)–As(2)–B(2)	108.1(3)
B(2)–C(37)	1.574(10)	Si(2)–As(2)–C(28)	108.9(2)
B(2)–C(46)	1.600(11)	As(2)–B(2)–C(37)	119.2(6)
		As(2)–B(2)–C(46)	118.3(5)
		C(37)–B(2)–C(46)	121.6(6)

PhB{As(*t*-Bu)$_2$}$_2$ (2). The molecular structure of **2**, which is represented in Figure 2, possesses no crystallographically imposed symmetry. The slightly different As(1)–B and As(2)–B bond lengths of 2.064(5) and 2.034(5) Å, respectively, correspond to small differences in pyramidicity at As(1) and As(2). The sums of angles at As(1) and As(2) are 316° and 320°. The angles between the perpendiculars to the C(15)–As(1)–C(19) and C(1)–B–As(2), and the C(7)–As(2)–C(11) and C(1)–B–As(1) planes are 39.4° and 26.9°. The B–C bond length is 1.562(7) Å, and the As–C bonds span the range 2.026(4)–2.047(5) Å. The boron has planar coordination with angles in the range 114.0(2)–124.3(3)°. The angle between the plane at boron and the phenyl ring is 79.7°.

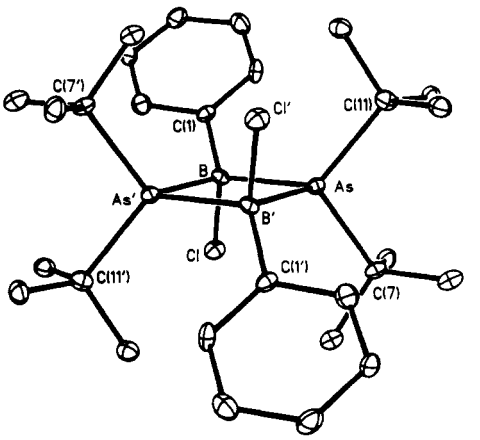

Figure 1. Computer-generated thermal ellipsoid (30%) plot of **1**. Hydrogen atoms are omitted for clarity.

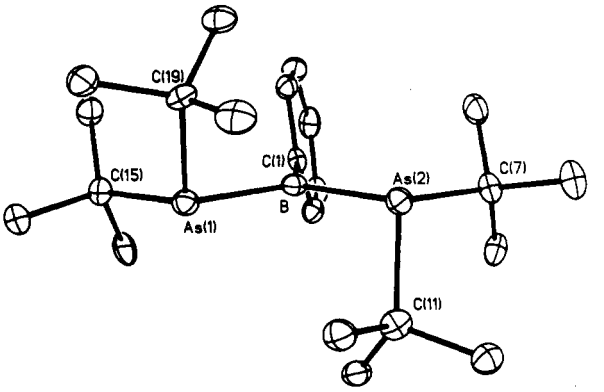

Figure 2. Computer-generated thermal ellipsoid (30%) plot of **2**. Hydrogen atoms are omitted for clarity.

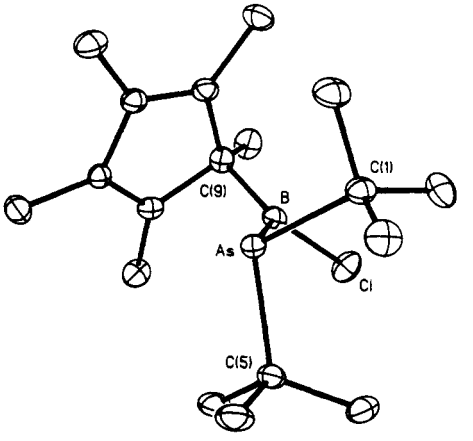

Figure 3. Computer-generated thermal ellipsoid (30%) plot of **3**. Hydrogen atoms are omitted for clarity.

Cp*B(Cl)As(*t*-Bu)$_2$ (3). The structure of the monomeric compound **3** is illustrated in Figure 3. The sum of angles at As is 312°, and the B–As bond length is 2.085(4) Å. The angle between the bisectors of the C(1)–As–C(5) and C(9)–B–Cl planes

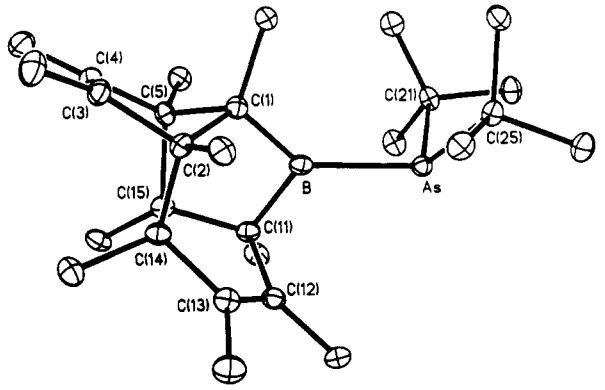

Figure 4. Computer-generated thermal ellipsoid (30%) plot of **4**. Hydrogen atoms are omitted for clarity.

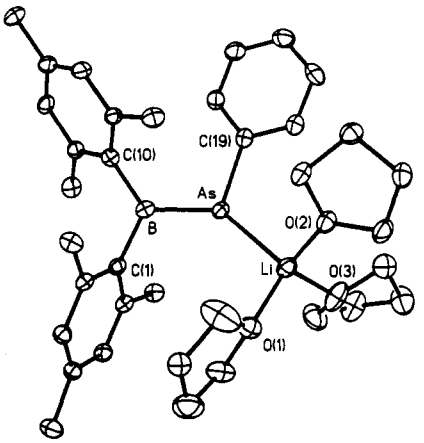

Figure 5. Computer-generated thermal ellipsoid (30%) plot of **5**. Hydrogen atoms are omitted for clarity.

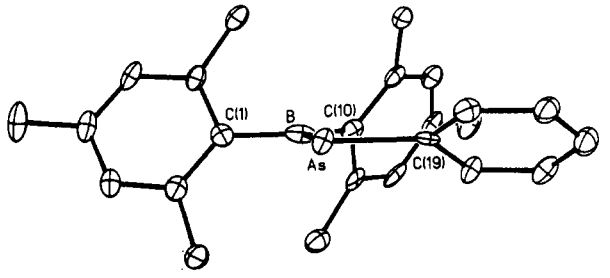

Figure 6. Computer-generated thermal ellipsoid (30%) plot of the anion for **6**. Hydrogen atoms are omitted for clarity.

is 71.7°. The boron has a planar coordination, and the B–C(9) and B–Cl bond lengths are 1.596(6) and 1.776(4) Å, respectively.

$(C_{20}H_{30})BAs(t\text{-}Bu)_2$ (4). The structure of **4** (Figure 4) is monomeric. The arsenic atom has pyramidal coordination with the sum of angles at arsenic equal to 322°. The B–As bond length is 2.084(5) Å, and the angle between the bisectors of the C(21)–As–C(25) and C(1)–B–C(11) planes is 60.2°. The data also show that there has been a [4 + 2] cycloaddition of the boron Cp* ligands. The structure illustrates the formation of two C–C single bonds, C(2)–C(14) and C(5)–C(15) which link the original Cp* rings. In addition, the C(12)–C(13) and C(3)–C(4) bond lengths are consistent with C–C double bonds. The extremely wide As–B–C(1) and narrow C(1)–B–C(11) angles, 136.2(2)° and 105.5(3)° at the planar coordinated boron, indicate the geometrical restriction imposed by the Diels–Alder addition of the Cp* ligands.

$Mes_2BAs(Ph)SiMe_3$ (7). The structure of **7** (Figure 7) has two chemically equivalent but crystallographically independent monomers that have very similar structure. The arsenic atoms are pyramidal in each molecule. The sums of angles at As(1) and As(2) are 322° and 323°. The As(1)–B(1) and As(2)–B(2) bond lengths are 2.031(8) and 1.999(8) Å. The angle between the bisectors of the Si–As–C and C–B–C planes are 18.9° in the case of As(1) and 22.4° for As(2). The average As–Si and As–C bond lengths are 2.365(3) and 1.947(7) Å, respectively. Coordination at the boron centers is planar, with angles at boron which vary from 116° to 124°. The average angle between the boron plane and the mesityl rings is 61.3°.

^{11}B and Variable Temperature ^1H NMR Studies. Table IV presents the ^{11}B NMR chemical shifts for compounds **1–7** and other related species. The new study involving variable-temperature ^1H NMR concerns compound **7**. A similar study of **5** was reported in a preliminary communication in which a barrier to rotation of 21 kcal mol^{-1} around the B–As bond was measured. Energy barriers (ΔG^*) for the dynamic processes were calculated by using an approximate formula.[23] In the case of **7** at 25 °C, well-resolved singlets were observed for the *m*-H, *o*-Me, and *p*-Me resonances. Increasing the temperature to 100 °C affords an unchanged spectrum. However, broadening and a concomitant decrease in intensity of the *o*-Me and *m*-H peaks were observed upon cooling the sample. The *o*-Me and *m*-H signals split into two singlets at about −15 and −25 °C, respectively. These coalescence temperatures together with the maximum peak separations (at −73 °C) of 238Hz and 78Hz for o-Me and m-H affords a consistent barrier of about 11.8 kcal mol^{-1} for the dynamic process.

Discussion

Synthesis. The synthesis of B–As compounds by conventional salt elimination routes is not always straightforward. Initial attempts at synthesizing such compounds involved reactions (usually in Et_2O solution) between lithium arsenides such as Ph_2AsLi and Ph(H)AsLi and dimesitylborylfluoride (Mes_2BF), a reagent that was used extensively in the synthesis of the analogous borylphosphides (Mes_2BPR_2).[3,5a,6,19] However, in some cases a mixture was obtained that often included boron–oxygen compounds and the Mes_2BF starting material.

For **1–4** it was found that the reaction between lithium arsenides and B–Cl precursors proceeded smoothly with LiCl salt elimination. Furthermore, the use of crowding substituents (Cp* = 1,2,3,4,5-Me_5C_5 and Mes = 2,4,6-$Me_3C_6H_2$) at boron in compounds **3–7** prevented the type of head-to-tail association observed in the structure of **1**. The synthesis of **1** was carried out with the intention of further substitution at boron by reaction with the second B–Cl moiety. Unfortunately, reaction of **1** with various RLi reagents in Et_2O (where R = *t*-Bu-, Mes-, Ph-) gave products that were not readily characterizable. In contrast, reaction with a second equivalent of *t*-Bu_2AsLi afforded the diarsinoborane **2** in good yield. Incomplete reaction and a mixture of products resulted from the synthesis of **3**. These products consistently included more than 60% recovery of the starting material Cp^*_2BCl. Presumably, the greater bulk at the boron center in **3** hinders the reaction. Further variation of the substituents at arsenic was accomplished by reaction of $Mes_2BAs(Ph)Li(THF)_3$ (**5**) with $ClSiMe_3$ to generate $Mes_2BAs(Ph)SiMe_3$ (**7**).

Structures. Compounds **2–7** are, apparently, the first structurally characterized molecular compounds with bonds between three-coordinate boron and arsenic substituted by non-π-interactive ligands. More surprisingly, perhaps, $[PhB(Cl)As(t\text{-}Bu)_2]_2$ (**1**) is the first structurally characterized dimeric arsinoborane species. The dimerization apparently results from inadequate kinetic stabilization of the monomer $[PhB(Cl)As(t\text{-}Bu)_2]$ by insufficiently bulky ligands. **1** crystallizes in the anti form, presumably because steric interactions are minimized. In solution, there is no evidence (^1H and ^{11}B NMR) of an equilibrium between

(23) Kost, D.; Carlson, E. H.; Raban, M. *J. Chem. Soc., Chem. Commun.* **1971**, 656.

Table III. Selected Structural Details for Compounds **1–7** and Other Related Compounds

	B–As (Å)	Σ°As (deg)[a]	twist angle (deg)[b]	ref
$[PhB(Cl)As(t\text{-}Bu)_2]_2$ (**1**)	2.200(5)			this work
	2.184(5)			
$PhB\{As(t\text{-}Bu)_2\}_2$ (**2**)	2.064(5)	316°	39.4°	this work
	2.034(5)	320°	26.9°	
$Cp^*B(Cl)As(t\text{-}Bu)_2$ (**3**)	2.085(4)	312°	71.7°	this work
$(C_{20}H_{30})BAs(t\text{-}Bu)_2$ (**4**)	2.084(5)	322°	60.2°	this work
$Mes_2BAsPhLi(THF)_3$ (**5**)	1.926(6)	341°	1.1° [c]	4
$[Mes_2BAsPh][Li(TMEDA)_2]$ (**6**)	1.936(11)	360°	1.1° [c]	4
$Mes_2BAs(Ph)SiMe_3$ (**7**)	2.031(8)	322°	18.9°	this work
	1.999(8)	323°	22.4°	
[–B(N*i*-Pr$_2$)-N(*t*-Bu)-B(N*i*-Pr$_2$)-As(Ph)-] (**8**)	2.063(4)	272°		11
	2.069(4)			

[a] Sum of the angles at As. [b] Defined as the angles between the perpendiculars to the R–As–R(R′) and R–B–R(R′) planes when viewed along the B–As bonds. [c] The interplanar angle between the C(1)–B–C(10) and As–B–C(19) planes.

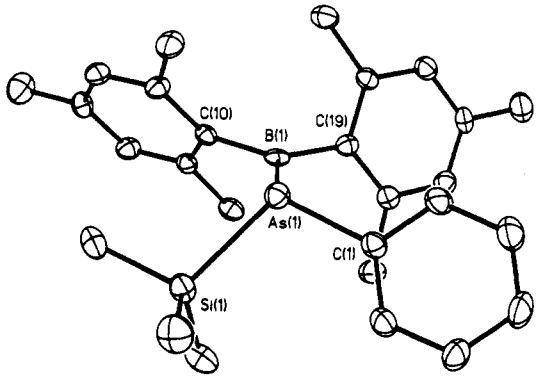

Figure 7. Computer-generated thermal ellipsoid (30%) plot of **7**. Hydrogen atoms are omitted for clarity.

Table IV. ^{11}B NMR Chemical Shift Values for **1–7** and Other Related Compounds

compound	^{11}B (ppm)[a,b]	ref
$[PhB(Cl)As(t\text{-}Bu)_2]_2$ (**1**)	83.0	this work
Me_3AsBBr_3[c]	–16.4	34
Me_3AsBI_3[c]	–38.1	34
$PhB\{As(t\text{-}Bu)_2\}_2$ (**2**)	107.6	this work
$Cp^*B(Cl)As(t\text{-}Bu)_2$ (**3**)	69.6	this work
$(C_{20}H_{30})BAs(t\text{-}Bu)_2$ (**4**)	52.1	this work
$Mes_2BAsPhLi(THF)_3$ (**5**)	74.6	this work
$[Mes_2BAsPh][Li(TMEDA)_2]$ (**6**)	74.9	this work
$Mes_2BAs(Ph)SiMe_3$ (**7**)[d]	92.5	this work
[–B(N*i*-Pr$_2$)-N(*t*-Bu)-B(N*i*-Pr$_2$)-As(Ph)-] (**8**)[d]	38.4	11

[a] Referenced to $BF_3{\cdot}Et_2O$. [b] In C_6D_6 unless otherwise stated. [c] In $CDCl_3$. [d] In C_7D_8.

the two forms.[24] The B–As bonds in **1** are quite long and are comparable to those observed in the closo icosahedral $MAs_2B_9H_8$ or 9 (where M = Pt or Pd)[8] cage structures. Shorter B–As bond lengths (2.03(1)–2.065(6) Å) were observed[9] in the structures of three trimethylarsine–boron trihalide adducts, Me_3AsBX_3 (where X = Cl, Br, or I). This bond shortening may be attributed, perhaps, to the higher Lewis acidity of the boron trihalides. At the same time, the greater size of the substituents in **1** may lengthen the B–As bond. The shorter B–As bond lengths in **2–7** can be explained mainly by the dissimilarity of coordination (at boron and arsenic, 3 vs 4), hybridization (primarily at boron, sp^2 vs sp^3), and, in some cases (vide infra), B–As p–p π-bonding.

Compound **2** is related to the phosphorus compound $PhB(PMes_2)_2$,[5b] both of which may be regarded as analogues of the allyl anion. Not surprisingly, **2** and $PhB(PMes_2)_2$ have similar structural features. The arsenics have pyramidal coordination, and there is a close correlation between the B–As bond lengths, the degree of pyramidicity at As, and the twist angle between the lone pair of arsenic and the empty p-orbital of boron. The shorter B–As bond is found with the less pyramidal As center and the smaller twist angle. Furthermore, the geometries at arsenic are more flattened than in $AsPh_3$ (Σ°As = 299°).[25] This is consistent with some B–As π-bonding, although the B–As distances are not much shorter than the predicted single bond length. However, since the phosphorus analogue has flatter P geometries and slightly shortened B–P bonds,[5b] the differences between the two species may be due to the higher inversion barrier at As.[14]

In the arsinoboranes **3** and **4**, arsenic and boron are present in a one-to-one ratio, which allows a direct assessment of B–As π bonding in the absence of competing ligands on boron. The structural data suggest an absence of significant B–As multiple bonding. Like the related monomeric arsinogallanes $Cp^*_2GaAs(SiMe_3)_2$[26] and $(t\text{-}Bu)_2GaAs(t\text{-}Bu)_2$,[27] **3** and **4** (see Table III) feature large twist angles (>60°) between the lone pair of arsenic and the empty p-orbital on boron and strongly pyramidal coordination at arsenic. Enhancement of the π-bonding in **3** might have been expected since data for related phosphorus compounds of formula $XB(PMes_2)_2$ (where X = OEt or Br) show that B–P multiple bonding is increased by electron-withdrawing substituents on boron.[28] However, the long B–As distances (~2.085 Å) of **3** and **4** are almost identical. Presumably, these bond lengths (slightly greater than the sum of atomic radii by ~0.025 Å) reflect the greater steric requirements of the Cp ligands as well as the absence of significant B–As p–p π-overlap. A weak interaction in **3** between the As lone pair and the π^*-system of the Cp* ligand as indicated by the orientation in Figure 3 is not supported by the As···Cp* centroid distance of ~3.05 Å. A concomitant lengthening of the C=C bonds (~1.355 Å) in the Cp* diene ring might have been expected, but this is also not observed. The remarkable structure of **4** is probably a result of steric congestion which induces a [4 + 2] cycloaddition of the boron Cp* ligands. To our knowledge, this represents the first structurally characterized example of a cycloaddition between two Cp* units. It is possible that the additional bulk of -As(*t*-Bu)$_2$ at boron forces the Cp* ligands together, allowing Cp* HOMO–LUMO interactions to occur. The reaction conditions, which involved an overnight reflux, may have driven the thermally allowed cycloaddition.

The lithium borylarsenide salts **5** and **6** and the silyl-substituted compound **7** were synthesized to investigate the effect of electropositive substituents on B–As bonding. The structures (X-ray) of previously communicated **5** and **6** offer strong evidence for B–As π-bonding.[4] In contrast to compounds **1–4** and **7**, the B–As distances in **5** and **6** (~1.93 Å) are extremely short. In addition, there is a nearly planar C_2B–As–C core array in each case. Some of the contraction in the B–As bond lengths is, of

(24) An equilibrium between the syn and anti forms of the Ga–P dimer $[t\text{-}Bu_2Ga(\mu\text{-}(C_5H_9)PH)]_2$ (anti form in the solid state) was shown to exist in solution by ^{31}P NMR: Heaton, D.E.; Jones, R. A.; Kidd, K. B.; Cowley, A. H.; Nunn, C. M. *Polyhedron* **1988**, *7*(19/20), 1901.

(25) Haque, M. U.; Tayim, H. A.; Ahmed, J.; Horne, W. *J. Crystallogr. Spectrosc. Res.* **1985**, *15*(6), 561.

(26) Byrne, E. K.; Parkanyi, L.; Theopold, K. H. *Science* **1988**, *241*, 332.

(27) Higa, K. T.; George, C. *Organometallics* **1990**, *9*, 275.

(28) Karsch, H. H.; Hanika, G.; Huber, B.; Meindl, K.; König, S.; Kruger, C.; Muller, G. *J. Chem. Soc., Chem. Commun.* **1989**, 373.

course, due to a change in σ-hybridization. This shortening, however, is probably no more than 0.05 Å, which implies that the π-bond along with some ionic contribution is responsible for the remaining 0.1 Å of the contraction.[29] Strong evidence for π-bonding also comes from the variable-temperature ^{1}H NMR data for **5**, which yielded a rotation barrier of 21 kcal mol^{-1}. This high value is comparable to those observed in the analogous B–P and B–N systems.[6,30] In the silyl-substituted **7**, the B–As distances (2.031(8) and 1.999(8) Å) in the two molecules in the asymmetric unit are shortened by ca. 0.05 Å. The coordinations at the arsenic atoms are flattened pyramidal ($\Sigma°$As $\sim$ 323°) as in **2–4**. Thus, the structural and variable-temperature ^{1}H NMR (vide infra) data indicate that B–As π-bonding in **7**, although present, is weaker than that in **5** or **6**.

The reasons for the dramatic changes in the B–As bonding in **5** and **6** are connected to the effects of electropositive substituents on inversion barriers. Replacement of the organic groups at arsenic by lithium leads to an increase in the electron density on arsenic[31] which results in a decrease in the inversion barrier at arsenic through stabilization of the planar transition state.[32] This leads to a strengthening of the B–As π-interaction through more efficient orbital overlap. The interaction between Li^+ and the anion is primarily ionic, and this is confirmed by the complete separation of Li^+ that is observed when TMEDA is added to **5**. Removal of the Li^+ has little effect on the B–As bond length, and the deviation of the Li–As vector from the molecular plane in **5** is thus not indicative of a weak π-bond. The deviation appears to be primarily determined by steric factors and perhaps crystal packing forces. The comparatively short As–C distances in **5–7** may be attributed to the sp^2 hybridization of the ipso phenyl carbon. In addition, the As–Si distances observed in **7** agree well with the sum of the As (1.21 Å) and tetrahedral Si (1.18 Å) radii.[12]

NMR Studies. A variable-temperature (VT) ^{1}H NMR study was undertaken to investigate the strength of possible B–As multiple bonding in **7**. Observation of the behavior of two sets of proton resonances yielded two independent but identical barriers of 11.8 kcal mol^{-1}. This dynamic process may be assigned to either restricted rotation aroundthe B–As bond as in **5** or to an aromatic ring flip. Both possibilities have to be borne in mind since VT ^{1}H NMR studies of arylboryloxides such as Mes_2-BOMe[33] have given barriers as high as 12 kcal mol^{-1} which were assigned to a ring flip of the Mes groups.[34] It is notable, however, that no splitting of the *p*-Me signal is observed upon cooling. This suggests that the dynamic process is the ring flip. However, one of the peaks, attributable to the *o*-Me or *m*-H groups, is much broader than the other, suggesting another dynamic process that may be associated with restricted rotation around the B–As bond. This uncertainty notwithstanding, it is possible to say that the upper limit of the strength of π-bonding in **7** is ca. 10–12 kcal mol^{-1}, which is approximately half of that observed in **5**.

As with the phosphinoboranes, the ^{11}B NMR chemical shifts of the arsinoboranes are not highly sensitive to the changes in B–As multiple bond character (see Table IV). The observed ^{11}B shift values for **2–8** of 38–108 ppm are within the range expected for three-coordinate boron compounds.[34] The upfield shift for the cyclic species **8** may be attributed to enhanced electron density at boron due to π-bonding from the amino groups. The downfield shift for **1** is somewhat unexpected, in view of the shifts of the four-coordinate Me_3AsBX_3[34] derivatives. It may arise from lower electron density at boron owing to the weakness of the B–As bonds. The mixture of compounds obtained during the synthesis of **3** was also monitored by ^{11}B NMR. A major peak is that of unreacted Cp^*_2BCl at δ 72.[17] In addition to the signal for **3**, (i.e., δ 52.1), two other resonances appear at δ 31.4 and 7.35. The minor peak at 31.4 ppm may be from boron–oxygen impurities (e.g., $(Cp^*BO)_{2\text{ or }3}$ or $Cp^*B(OH)_2$) which were also detected in the syntheses of many B–P compounds.[6] This may be due to reaction with the ether solvent or small amounts of moisture. The shift is similar to that of $Cp^*B(OMe)_2$, δ 29.5[17] and (n-C_4H_9-BO)$_3$, δ 32.5.[35] The upfield peak at δ 7.35 may be due to a four-coordinate boron species.[34]

Acknowledgment. We thank the National Science Foundation for financial support.

Supplementary Material Available: Analytical and spectroscopic data; tables of data collection parameters, bond distances and angles, hydrogen coordinates, and anisotropic thermal parameters (45 pages); list of observed and calculated structure factors (68 pages). Ordering information is given on any current masthead page.

(29) Pestana, D. C.; Power, P. P. *Inorg. Chem.* **1991**, *30*, 528.
(30) Barfield, P. A.; Lappert, M. F.; Lee, J. *Trans. Faraday Soc.* **1968**, *64*, 2571.
(31) (a) Baechler, R. D.; Mislow, K. *J. Am. Chem. Soc.* **1970**, *92*, 4758; (b) *J. Am. Chem. Soc.* **1971**, *93*, 773.
(32) Levin, C. C. *J. Am. Chem. Soc.* **1975**, *97*, 5649.
(33) Finocchiaro, P.; Gust, D.; Mislow, K. *J. Am. Chem. Soc.* **1973**, *95*, 7029.
(34) Nöth, H.; Wrackmeyer, B. *Nuclear Magnetic Resonance Spectroscopy of Boron Compounds*; Springer Verlag: Berlin 1978; and references therein.